Chemical Engineering Journal 141 (2008) 346–353

Contents lists available at ScienceDirect

Chemical Engineering Journal

journal homepage: www.elsevier.com/locate/cej

Variable-property effect on liquid flow and heat transfer in microchannels

J.T. Liu, X.F. Peng*, B.X. Wang

Laboratory of Phase Change and Interfacial Transport Phenomena, Department of Thermal Engineering, Tsinghua University, Beijing 100084, China

ARTICLE INFO

Article history:
Received 15 November 2007
Received in revised form 17 February 2008
Accepted 25 February 2008

Keywords:
Convection
Microchannel
Temperature-dependent property
Flow and thermal re-development

ABSTRACT

Numerical investigation was conducted in an effort to verify the variable-property effect of thermally developing flow in microchannel cooling passages. Temperature-dependent viscosity and thermal conductivity of liquid water were taken into account in theoretical modeling. Two-dimensional simulation was performed for low Reynolds number flow in a 100 μm single channel subjected to localized heat flux and different inlet temperatures. The fundamental characteristics of flow and thermal re-development were carefully analyzed. The heat transfer enhancement was described by defining the peak value and location of relative Nusselt number distribution as $\Delta Nu\%_{max}$ and X_{max}. Strong non-linear interaction mechanism prevailed in the correlation of $\Delta Nu\%_{max}$ and X_{max} due to high heat flux condition and dramatic rise of liquid temperature.

1. Introduction

Fluid flow in microchannels is a widely studied topic due to its critical importance in a large variety of engineering applications and scientific disciplines, such as microscale heat exchangers and reactors used in electronics, automotive vehicles, biochemistry, laser process equipments, and aerospace technology, etc. Some early work includes Tuckerman and Pease [1], and Wu and Little [2,3]. And intensive investigations were performed experimentally and theoretically in the following decades [4–10].

The practical operation of microchannel devices, especially for liquids as working fluids, is generally characterized with low Reynolds number flow and high heat flux. One consequence of such conditions is the large variation of liquid properties, at least the viscosity and thermal conductivity, due to steep temperature gradient. Then the momentum equation is no longer independent of the energy equation in the conservative model, drawing significant difficulty in the theoretical analysis. Traditionally, the property-ratio method and reference temperature method [11] used to be employed to the correction of Nusselt number for convection in conventional tubes. Due to the empirical nature of the two methods, an asymptotic theory method was proposed by Herwig [12] as a theoretic reinforcement. Since the AT method was based on a linear temperature-dependence of the properties, it failed to provide reasonable prediction at large heat flux.

More robust treatment on the variable-property flow and heat transfer problems was implemented by the mature development of modern computation technology, e.g., the computational fluid dynamics and numerical heat transfer methods. In the last decade, the effects of temperature-dependent fluid property were emphasized in many micro- and pore-scale numerical researches, among which several latest studies are introduced briefly.

Nonino et al. [13] performed a parametric investigation on the effects of temperature-dependent viscosity in simultaneously developing laminar flow of a liquid in straight ducts. For ducts of five different cross-section shapes, the numerical results showed that the effects of temperature-dependent viscosity were non-negligible on laminar forced convection within a wide range of operative conditions. They further investigated the important role of viscous dissipation in a similar application in their recent publication [14]. Kumar et al. [15] studied the heat transfer and fluid flow with temperature-dependent properties in helical coil tubes at low-Reynolds number regime. The variation in thermophysical properties of water and diethylene glycol showed marked impact on the friction factor and Nusselt number, as well as the secondary flow profile. In their study of steady laminar-boundary-layer flow over an isothermal moving flat plat in the presence of a magnetic field, Seddeek and Salem [16] found that the variable viscosity effect has to be taken into consideration when the fluid viscosity is highly dependent on temperature. Pantokratoras [17] numerically investigated the steady laminar flow in a fluid-saturated porous medium channel between two parallel plates, concerning engine oil, water and air, with the variation of their physical properties with temperature. It was found that the temperature-dependent

* Corresponding author. Tel.: +86 10 6278 9751; fax: +86 10 6278 9751.
E-mail address: pxf-dte@mail.tsinghua.edu.cn (X.F. Peng).

1385-8947/$ – see front matter © 2008 Elsevier B.V. All rights reserved.
doi:10.1016/j.cej.2008.02.014

Nomenclature

Br_{qw}	Brinkman number based on wall heat flux
Br_{Sk}	modified Brinkman number based on viscosity–temperature sensitivity
$Br_{S\mu}$	modified Brinkman number based on thermal-conductivity–temperature sensitivity
c_p	specific heat (J/kg K)
D	channel width (m)
Eu	Euler number
h	heat transfer coefficient (W/m^2 K)
k	thermal conductivity (W/m K)
L	length (m)
Nu	local Nusselt number
p	pressure (N/m^2)
p_a	atmosphere pressure (N/m^2)
P	dimensionless pressure
Pr	Prandtl number
q''_w	wall heat flux (W/m^2)
Re_D	Reynolds number
S_k	thermal-conductivity–temperature sensitivity (W/m K^2)
S_μ	viscosity–temperature sensitivity (kg/ms K)
T	temperature (K)
u	main-flow velocity (m/s)
U	dimensionless main-flow velocity
w	cross-flow velocity (m/s)
W	dimensionless cross-flow velocity
x	axial coordinate (m)
X	non-dimensionalized abscissa by D
z	transverse coordinate (m)
Z	non-dimensionalized transverse coordinate by D

Greek letters

δ_t	thermal boundary layer thickness
θ	dimensionless temperature
μ	viscosity (kg/ms)
ρ	density (kg/m^3)
Φ	viscous dissipation term (W/m^3)

Subscripts

b	bulk
c	center
CP	constant property
DN	downstream region
FD	fully developed flow
H	heated region
m	mean
max	maximum
ref	reference
UP	upstream region
VP	variable property
w	wall
0	inlet property

Superscript

*	dimensionless form of selected parameter

viscosity and, in some cases, density and thermal conductivity played important roles when the temperature difference between the plates was large.

Apparently it does not require too much effort to apply temperature-dependent properties into complex mathematical and physical models at the aid of advanced computers. The fundamental mechanisms of the variable-property effect on basic mass and energy transportation, on the other hand, need to be understood based on rather simple models. Among many pioneer studies within this category, Mahulikar and Herwig [18–20] conducted a series of work to establish a continuum-based model for laminar convections in circular tube, incorporating with temperature dependence of fluid viscosity and thermal conductivity. They identified the physical effects due to the variation of viscosity and thermal-conductivity of liquid, and showed significant axial velocity profile distortion and radial flow due to viscosity variation, as well as axial conduction due to thermal-conductivity variation. Based on a similar theoretical model, Liu et al. [21] conducted numerical investigation on variable-property laminar convection study in microchannel under 2D Cartesian coordinates. They presented the single-hump-shaped distribution of local relative Nusselt number enhancement due to property variation, and further clarified the role of inlet Reynolds number. The axial conduction due to thermal-conductivity variation showed relatively low significance, simply because the Peclet number was larger than 50 within the operation range of their study.

As reported by previous researchers, the temperature-dependence of liquid properties introduced marked flow and thermal re-development, as well as heat transfer enhancement. Therefore both the heating condition and the initial status of liquid at the inlet should be of significant influence. As a step forward of previous study, the present work took inlet temperature as a parameter besides wall heat flux, and numerically investigated the two-dimensional low Reynolds number convection of liquid water in microchannels. A quantitative effort was performed on describing the Nusselt number enhancement behavior, as well as a theoretical analysis in details.

2. Description of problem

2.1. Fundamental consideration

Thermally developing and hydrodynamically developed flow is commonly encountered in the practical microchannel heat sinks and other associated applications, due to non-uniform heating conditions in terms of space and time scales. The problem is also termed as thermal entrance problem, or Graetz-type problem, following the first work by Graetz [22] in 1883 and Nusselt [23] in 1910. Only energy equation is solved in the classical treatment of this kind of problem, by assuming unchanged parabolic velocity profile along the flow. However, in the variable-property thermal entrance problem, as investigated in present work, the flow and energy equations are fully coupled with each other through the temperature-dependent viscosity. Therefore, both hydrodynamic and thermal boundary development take place along the heated channel, regardless of fully developed inlet velocity condition. For the convenience of discussion, a two-dimensional model is set upon a two-parallel-plate domain, with equations and boundary conditions specified in the following sections.

2.2. Equations and boundary conditions

The mathematical descriptions are derived from continuum-based conservation equations of mass, momentum and energy [24], incorporating with the following several important assumptions:

(1) Incompressible Newtonian fluid and steady laminar flow.
(2) Constant specific heat of the fluid.
(3) Thermal conductivity and viscosity are the single variable functions of temperature.
(4) Negligible effect of gravity and other body forces.

Since the discussion is restricted within two-dimensional Cartesian coordinates, the non-dimensional governing equations are derived in the following forms:

Continuity equation:

$$\frac{\partial U}{\partial X}+\frac{\partial W}{\partial Z}=0 \tag{1}$$

X-component momentum equation:

$$U\frac{\partial U}{\partial X}+W\frac{\partial U}{\partial Z}=-Eu\frac{\partial P}{\partial X}+\frac{\mu^*}{Re_D}\left(\frac{\partial^2 U}{\partial X^2}+\frac{\partial^2 U}{\partial Z^2}\right)+\frac{1}{Re_D}\frac{Br_{S\mu}}{Br_{qw}}S_\mu^* \times\left[2\frac{\partial\theta}{\partial X}\frac{\partial U}{\partial X}+\frac{\partial\theta}{\partial Z}\left(\frac{\partial U}{\partial Z}+\frac{\partial W}{\partial X}\right)\right] \tag{2}$$

Z-component momentum equation:

$$U\frac{\partial W}{\partial X}+W\frac{\partial W}{\partial Z}=-Eu\frac{\partial P}{\partial Z}+\frac{\mu^*}{Re_D}\left(\frac{\partial^2 W}{\partial X^2}+\frac{\partial^2 W}{\partial Z^2}\right)+\frac{1}{Re_D}\frac{Br_{S\mu}}{Br_{qw}}S_\mu^* \times\left[\frac{\partial\theta}{\partial X}\left(\frac{\partial W}{\partial X}+\frac{\partial U}{\partial Z}\right)+2\frac{\partial\theta}{\partial Z}\frac{\partial W}{\partial Z}\right] \tag{3}$$

Energy equation:

$$U\frac{\partial\theta}{\partial X}+W\frac{\partial\theta}{\partial Z}=\frac{1}{Re_D Pr}\left\{k^*\left(\frac{\partial^2\theta}{\partial X^2}+\frac{\partial^2\theta}{\partial Z^2}\right)+\frac{Br_{Sk}}{Br_{qw}}S_k^*\left[\left(\frac{\partial\theta}{\partial X}\right)^2+\left(\frac{\partial\theta}{\partial Z}\right)^2\right]+\Phi^*\right\} \tag{4}$$

The dimensionless parameters in Eqs. (1)–(4) are defined as below:

$$\mathbf{R}=X\mathbf{e}_i+Z\mathbf{e}_k=\frac{\mathbf{r}}{D}=\frac{x\mathbf{e}_i}{D}+\frac{z\mathbf{e}_k}{D},\quad \mathbf{U}=U\mathbf{e}_i+W\mathbf{e}_k=\frac{\mathbf{u}}{u_0}=\frac{u\mathbf{e}_i}{u_0}+\frac{w\mathbf{e}_k}{u_0},$$
$$\theta=\frac{k_0(T-T_0)}{q''_w D},\quad k^*=\frac{k}{k_0},\quad \mu^*=\frac{\mu}{\mu_0},\quad P=\frac{p}{p_a},\quad S_\mu^*=\frac{S_\mu}{S_{\mu,0}},\quad S_k^*=\frac{S_k}{S_{k,0}}, \tag{5}$$
$$Re_D=\frac{\rho u_0 D}{\mu_0},\quad Pr=\frac{c_p\mu_0}{k_0},\quad Eu=\frac{p_a}{\rho u_0^2},\quad Br_{qw}=\frac{u_0^2\mu_0}{q''_w D},\quad Br_{S\mu}=\frac{S_{\mu,0}u_0^2}{k_0},\quad Br_{Sk}=\frac{S_{k,0}\mu_0 u_0^2}{k_0^2}$$

And Φ^* stands for the viscous dissipation term:

$$\Phi^*=Br_{qw}\mu^*\left[2\left(\frac{\partial U}{\partial X}\right)^2+2\left(\frac{\partial W}{\partial Z}\right)^2+\left(\frac{\partial W}{\partial X}+\frac{\partial U}{\partial Z}\right)^2\right] \tag{6}$$

The dimensional parameters in Eqs. (1)–(4) are given as: $S_\mu = \mathrm{d}\mu/\mathrm{d}T$, the viscosity-temperature sensitivity; $S_k = \mathrm{d}k/\mathrm{d}T$, the thermal-conductivity-temperature sensitivity.

The physical significance of Brinkman numbers, Br_{qw}, $Br_{S\mu}$ and Br_{Sk} were elaborated in the work of Mahulikar and Herwig [18]. Therefore a rather brief introduction is presented here out of integrality purpose. The Br_{qw} is the Brinkman number based on wall heat flux, $Br_{S\mu}$ is modified Brinkman number based on viscosity-temperature sensitivity, and Br_{Sk} is modified Brinkman number based on thermal-conductivity-temperature sensitivity. In the dimensionless form of conservative equations, Br_{qw} appears as a multiplier to the viscosity dissipation term, while its reciprocal appears before the temperature terms that determine the significance of variation in fluid properties. For a typical application of microchannels, high heat flux and low flow velocity always result in small value of Br_{qw}, which indicates strong influence of property variation on the convection and negligible viscous dissipation term of Eq. (6). $Br_{S\mu}$ shows the relative importance of viscosity-variation induced cross-flow momentum transport over the energy transport due to the fluid conduction, while Br_{Sk} shows the relative significance of cross-flow momentum transport induced by thermal conductivity variation.

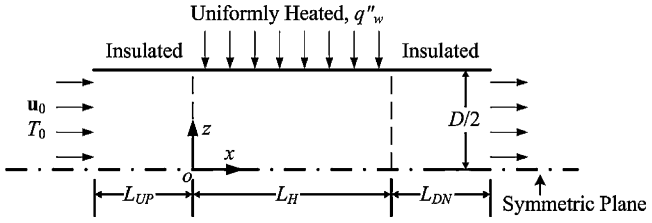

Fig. 1. Schematic diagram of analytical model.

The governing equations are solved in a two-dimensional domain shown in Fig. 1. Taking the advantage of symmetry, only a half of the channel is modeled. The channel wall is divided into three sections. The center region is heated at constant heat flux, q''_w, while the upstream and downstream regions are adiabatic walls. The length of heated region is fixed at 20D. The lengths of upstream and downstream region are both set as 10D, which are selected based on a compromise between computation cost and the requirement for numerical stability. No slip condition is set at walls of the three regions. The origin of the two-dimensional rectangular coordinate system is located at the start point of heated region on the centerline (symmetric plane), with the x-axis running along the channel.

At the entrance ($X=-10$), the hydrodynamically fully developed flow condition is assumed with uniform temperature (un-developed), given as:

$$U=1.5(1-4Z^2) \tag{7a}$$

$$W=0 \tag{7b}$$

$$\theta=0 \tag{7c}$$

At the exit ($X=30$), the axial gradients for all the transport variables except pressure are assumed to be zero.

2.3. Properties

Water is used as working liquid in this simulation within the temperature range of liquid phase at atmospheric pressure, i.e., from 0 to 100 °C. The temperature dependency of viscosity for liquid water is given as [24]:

$$\mu(T)=\mu(T_{ref})\left(\frac{T}{T_{ref}}\right)^n \exp\left[B(T^{-1}-T_{ref}^{-1})\right] \tag{8}$$

where $n=8.9$, $B=4700$ K, $\mu(T_{ref})=1.005\times10^{-3}$ kg/ms, $T_{ref}=293$ K. The temperature-dependent thermal conductivity is given by a cubic polynomial fitting result of data [25] in the following form:

$$k(T)=a_0+a_1T+a_2T^2+a_3T^3 \tag{9}$$

where $a_0=-1.135$, $a_1=0.01154$, $a_2=-2.375\times10^{-5}$ and $a_3=1.571\times10^{-8}$.

2.4. Numerical method and validation

The governing equations with boundary conditions were solved by the commercial CFD code, CFX5. The governing equations were

discretized by means of a fully implicit second order finite volume method with modified upwind advection scheme. In this work, the grid points used in the x- and z-directions were selected to be 600 and 70, respectively, with carefully distributed density near the central heated region. Effects of the grid number on the simulation accuracy were examined and the maximum deviations of predicted local Nusselt number were less than 0.014% among the computations on the grids of 240×50, 600×50, 600×70, 600×100 and 900×70. Therefore, the grid system of 600×70 points seemed to be sufficient to resolve the behaviors of the fluid flow and heat transfer in microchannels. A converged solution was obtained using this grid, with root mean square residuals less than 10^{-7} for all the transport variables and independent of the iteration numbers, and domain imbalances of mass, momentum and energy conservation less than 10^{-7}.

The validation of the numerical method was performed using water with constant properties and uniform heat flux condition over the entire channel wall, as a benchmark case. The temperature profile in the fully developed region of the channel showed excellent agreement with analytical solution. The Nusselt number obtained from simulation agreed with the theoretical value, $Nu_{CP,FD} = 70/17$ [26] with an relative error lower than 0.05%.

Apparently, the solution method and the formulation adopted were appropriate for the present study. For all investigated cases, the channel width, D was 100 μm, and inlet velocity $u_0 = 0.455$ m/s. Inlet temperature and heat flux varied within the range of 20–70 °C and $3–9 \times 10^5$ W/m^2, respectively. Converged results were obtained, as discussed in the next section.

3. Flow and thermal re-development

3.1. Velocity and temperature field characteristics

The streamwise development of main-flow velocity, U, and its gradient is drawn at the centerline of the channel (symmetric plane) in Fig. 2. The centerline velocity keeps the value of 1.5 for $X < 0^-$, since the fully developed flow condition is given at the domain inlet. When the flow enters the heated region ($X > 0^+$), due to high heat flux, dramatic spatial μ-variation takes place and distorts the parabolic U–Z profile. Such developing process could be clearly seen in Fig. 3, showing U–Z profile at different streamwise locations. The distorted profile varies together with temperature increase as the fluid heated along the flow until it achieves a most flattened profile (approximately $X = 13$). Afterward the flow undergoes a slowly recovering process towards the parabolic profile until it leaves the heated region and accelerates to achieve fully developed flow at the absence of heating. This flow development is quite different, or rather opposite to that of normal entrance problems, since the velocity profile develops outward to the channel wall and induces cross-flow velocity W to satisfy the local mass conservation (Eq. (1)). It is hereafter named 'flow re-development' in present work to distinguish the property-variation caused developing process from ordinary constant-property entrance problems. The re-developing flow enhances convection by introducing steeper velocity gradient adjacent to the wall. Additionally, transverse convection is also involved as an enhancement to the heat removal from the wall, in the term of $W(\partial\theta/\partial Z)$ in Eq. (4).

Regarding to the temperature distribution, it is generally believed that the thermal boundary layer thickness indicates the scale of temperature gradient across the flow and thus directly determines local heat transfer performance. In present work, the thermal boundary layer thickness, δ_t, is defined as the dimensionless distance from wall to the cross-sectional location where $(T_w - T)/(T_w - T_c) = 0.999$. The developments of δ_t are depicted in Fig. 4 for variable- and constant-property flows, where the solid curve stands for variable-property flow and the dash-dot curve stands for constant-property flow. It is noticeable that the two curves very well overlap with each other, except for the beginning part of heated region with slight departure. The cross-section temperature profiles are drawn at three typical streamwise locations, i.e., $X = 1$, 5 and 9. At the vicinity of the front of heated region ($X = 1$), variable-property temperature profile coincides with its constant-property counterpart along the flow section. As the fluid flows downwards, the two profiles begin to depart at the channel wall, but still merge into one curve near the centerline. For variable-property flow, the thermal conductivity is directly proportional to temperature for liquid water, thus $k_{w,VP} > k_0$ for high temperature near the wall. For constant-property flow, however, there is $k_{w,CP} = k_0$ at every location. Comparing the variable- and constant-property cases at same heat flux and x-location, since $q''_w = k_{w,VP}(\partial T/\partial Z)_{w,VP} = k_{w,CP}(\partial T/\partial Z)_{w,CP}$, there should be $(\partial T/\partial Z)_{w,VP} < (\partial T/\partial Z)_{w,CP}$. Additionally, Fig. 4 also shows that $T_{w,VP}$ is always lower than $T_{w,CP}$. The wall temperature difference $(T_{w,CP} - T_{w,VP})$ varies along the flow and exists even when thermal boundary layer thickness stops changing with streamwise location (approximately $X > 8$).

It is worth noting that, unlike the constant-property flow, there exist no "fully developed" flows for variable-property problem from either hydrodynamic or thermal point of view. This conclusion in flow aspect is straight forward since the main-flow velocity keeps changing with varying viscosity along the heated region. Regarding to the thermal aspect, on the other hand, it is slightly confusable due to the converging thermal boundary development. Such confusion is actually caused by the definition of δ_t. As long as the thermal conductivity varies with increasing fluid temperature, the cross-section temperature profile changes unceasingly along heated region and never achieves an unchanged "fully developed"

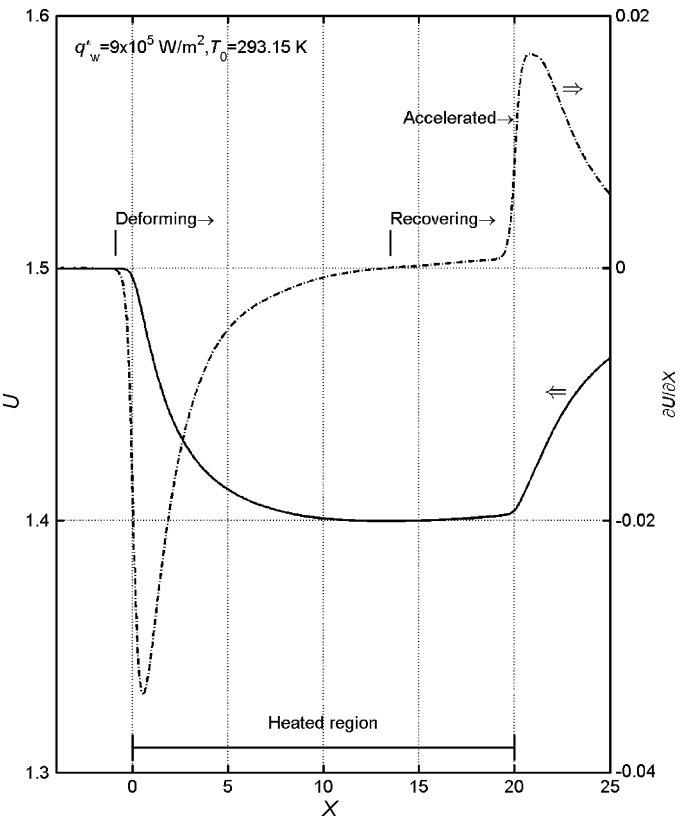

Fig. 2. Re-developing main-flow velocity and its streamwise gradient along X.

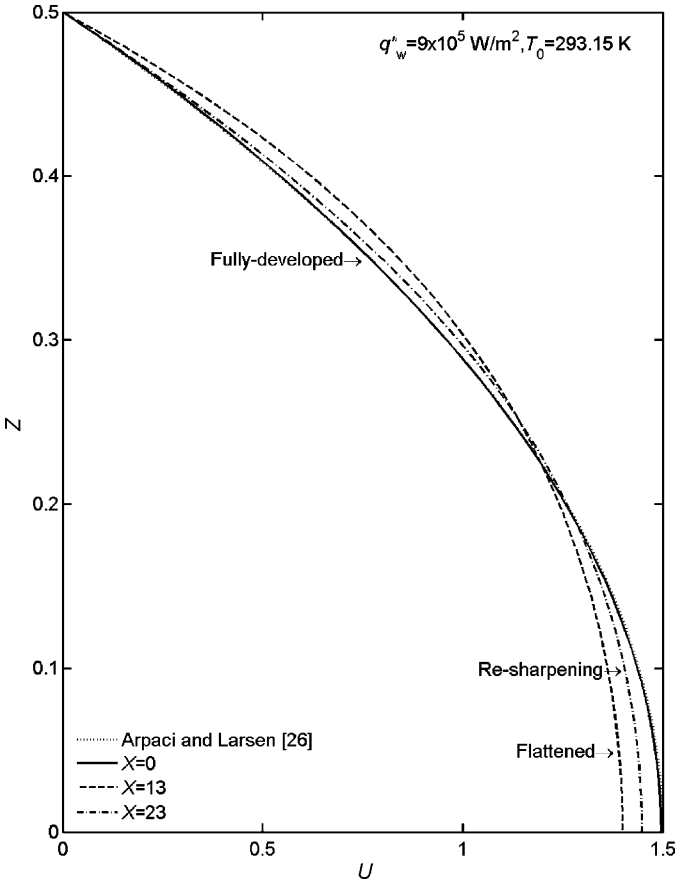

Fig. 3. Flow velocity profiles at different streamwise locations.

status. The concept of thermal boundary layer thickness, however, is unable to describe this variable-property phenomenon.

3.2. Heat transfer performance

Since the local heat transfer near the microchannel wall is the focused issue in present work, local Nusselt number shall be an important parameter, defined as:

$$Nu = \frac{hD}{k_m} = \frac{q''_w D}{k_m(T_w - T_b)} \tag{10}$$

where $T_b = \int_0^D \rho c_p u T \, dz / \dot{m} c_p = \int_0^D uT \, dz / u_m D$.

It is intuitive to predict a steep *Nu* jump near the front of heated region due to thin thermal boundary layer, regardless of variable- or constant-property flow, as hinted in Fig. 4. As the liquid flows downwards, the variable-property T_w begins to depart from the constant-property one. Since the bulk temperature, T_b is defined in terms of the thermal energy transported by the fluid as it moves past the cross section, $T_{b,VP}$ keeps the same value with $T_{b,CP}$ at each streamwise location and a same heat flux. Therefore, small $T_{w,VP}$ indicates higher heat transfer coefficient of variable-property flow than that of constant-property flow. The previous investigation [21] showed remarkable local Nusselt number increase in variable-property simulations, compared with constant-property results. This so-called variable-property effect was evaluated by the relative difference of local *Nu*, defined as follows:

$$\Delta Nu\% = \frac{Nu_{VP} - Nu_{CP}}{Nu_{CP}} \times 100 \tag{11}$$

Fig. 5 is a typical variable-property result showing the impact of heat flux on $\Delta Nu\%$ streamwise distributions at a specified inlet temperature. The $\Delta Nu\%$ curve starts from a low value at the immediate downstream of the front of heated region, and climbs up dramatically along the *X*-axis. The peak value of $\Delta Nu\%$ appears at a distance of 4–10*D* from *X*-origin. Afterward, the curve declines gradually downwards. As concluded previously [21], the relative enhancement of local Nusselt number due to variable-property effect is a strong function of heat flux. High heat flux results in a significant augment of $\Delta Nu\%$. Both the peak value and its location vary with the input heat flux as indicated by the up-arrows in Fig. 5.

The effect of inlet temperature is another concerned issue, which was rarely discussed in available investigations. As a similar phenomenon noted in Fig. 5, single-peaked $\Delta Nu\% \sim X$ curves are also presented in Fig. 6 for different inlet temperatures at a specified heat flux. The intensity and effective coverage of enhanced heat transfer are both affected by inlet temperature, lying in the fact that with increasing T_0, the peak value of $\Delta Nu\%$ curve declines, while the peak location moves downstream.

4. Variable-property effect

4.1. Correlations

The above-conducted observations and discussions imply that both q''_w and T_0 are important parameters on the variable-property enhancement of *Nu*, in respect of intensity and effective region. In seeking a mathematical description on this issue, rather than observation merely based on figures, two supplemental parameters, $\Delta Nu\%_{max}$ and X_{max}, denoting the peak value and location of

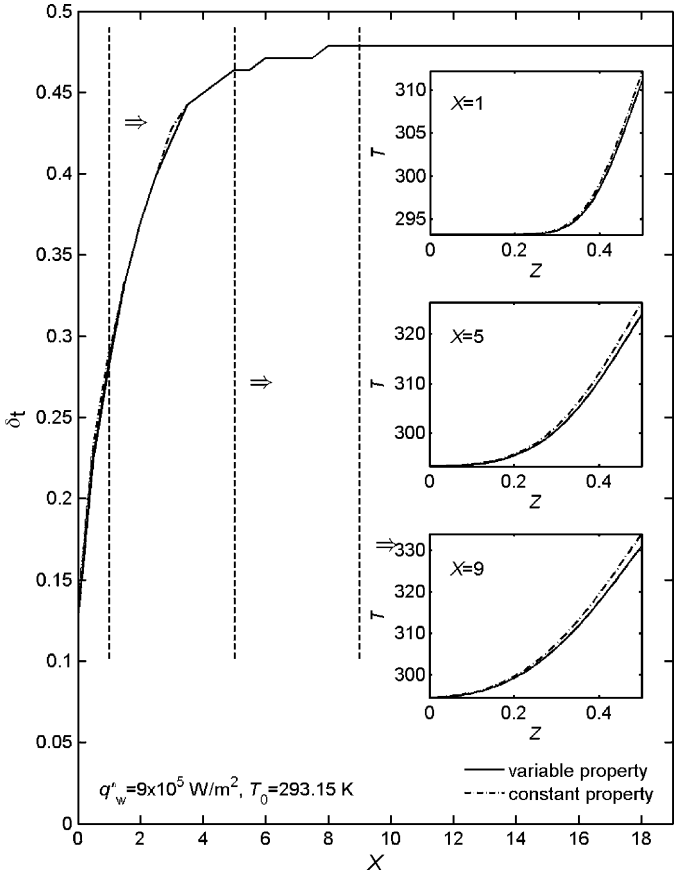

Fig. 4. Thermal development and cross-temperature profiles.

$\Delta Nu\% \sim X$ distribution, respectively, are introduced in describing the fundamental characteristics.

The $\Delta Nu\%_{max}$ data calculated from simulation results are shown in Fig. 7. For the same T_0, $\Delta Nu\%_{max}$ increases proportionally with increasing q''_w, whereas the impact of increasing T_0 results in declined $\Delta Nu\%_{max}$ for a specified heat flux. Both trends are clearly shown in Fig. 7(a), which are in consistency with the observation in Section 3.2. Since q''_w and T_0 are the concerned factors in present problem with other conditions unchanged, it naturally implicates the relation of $\Delta Nu\%_{max} = f(q''_w, T_0)$. For the convenience of discussion, the following form of function is boldly proposed, of which theoretical validation is examined later, as

$$\Delta Nu\%_{max} = C {q''_w}^A {T_0}^B \quad (12)$$

where A, B, and C are constants independent of q''_w and T_0.

A data processing procedure is carried out based on Eq. (12) and the three constants are calculated as $A = 0.8528$, $B = -4.695$, $C = 2.2158 \times 10^7$. Applying all conditions of q''_w and T_0 into Eq. (12) with the constants, predicted values of $\Delta Nu\%_{max}$ are compared with data from numerical results at corresponding conditions, as shown in Fig. 7(b). A maximum absolute value of relative error is obtained as low as 1.68%, indicating that the power-law form of function is compliant with the data characteristics, and that the processing procedure is under tight control of accuracy.

Fig. 8 shows the peak locations X_{max} of $\Delta Nu\% \sim X$ curves. A processing procedure is carried out to X_{max} data based on the assumed function form as

$$X_{max} = c {q''_w}^a {T_0}^b \quad (13)$$

The average constants are then obtained as $a = -0.3380$, $b = 2.796$ and $c = 5.8345 \times 10^{-5}$. As shown in Fig. 8(b), the prediction by Eq. (13) agrees well with the simulation data within a maximum absolute value of relative error as low as 4.18%.

The effects of q''_w and T_0 on X_{max} are clearly shown in Fig. 8(a). For a small value of X_{max}, peak value of Nusselt number enhancement appears near the beginning of heated region, indicating large effective region of variable-property effect. From this point of view, high heat flux not only results in increasing local heat transfer rate (high $\Delta Nu\%_{max}$ in Eq. (12)), but also achieves large coverage of the enhanced heat transfer (small X_{max} in Eq. (13)). Contrarily, high inlet temperature shows quite negative impact on variable-property effect in terms of weakened intensity as well as limited effective coverage.

4.2. Theoretical approach

Till now the relation between $\Delta Nu\%$ peak value and boundary conditions is empirically suggested as Eq. (12). From the definition of Nu and $\Delta Nu\%$ (Eqs. (10) and (11)), it is not difficult to derive the following expression:

$$\Delta Nu\% = \frac{k_0 (T_w - T_b)_{CP}}{k_m (T_w - T_b)_{VP}} - 1 \quad (14)$$

Note that in constant-property flow both the thermal conductivity and $(T_w - T_b)$ keep the same value for a specified heat flux and inlet temperature. In variable-property flow, on the other hand, k_m and $(T_w - T_b)$ vary along the channel, resulting in the X-dependent $\Delta Nu\%$ behavior. The viscosity variation is also involved through

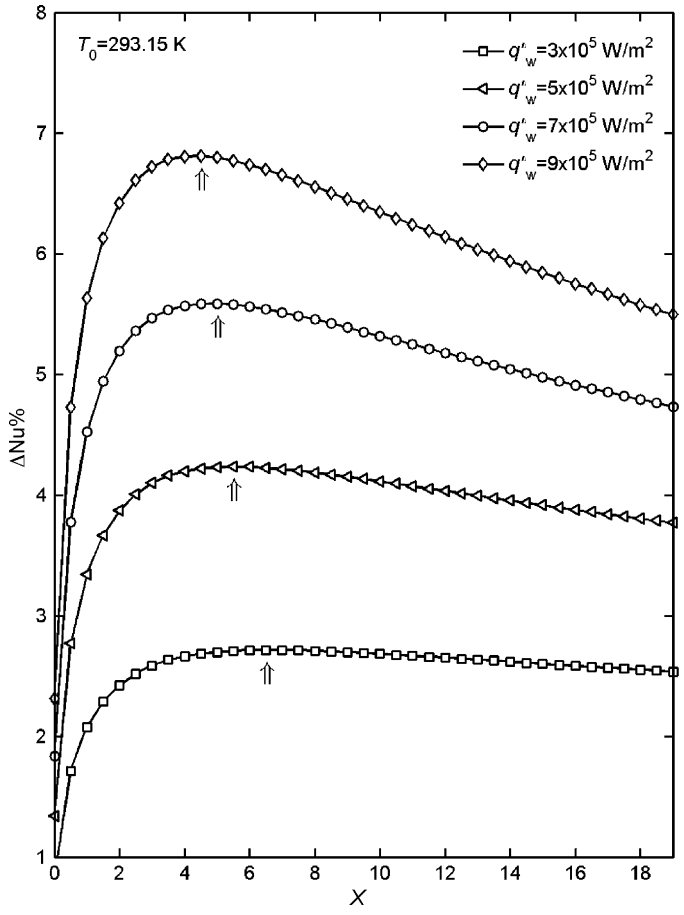

Fig. 5. Effects of heat flux q''_w on local $\Delta Nu\%$ at $T_0 = 293.15$ K.

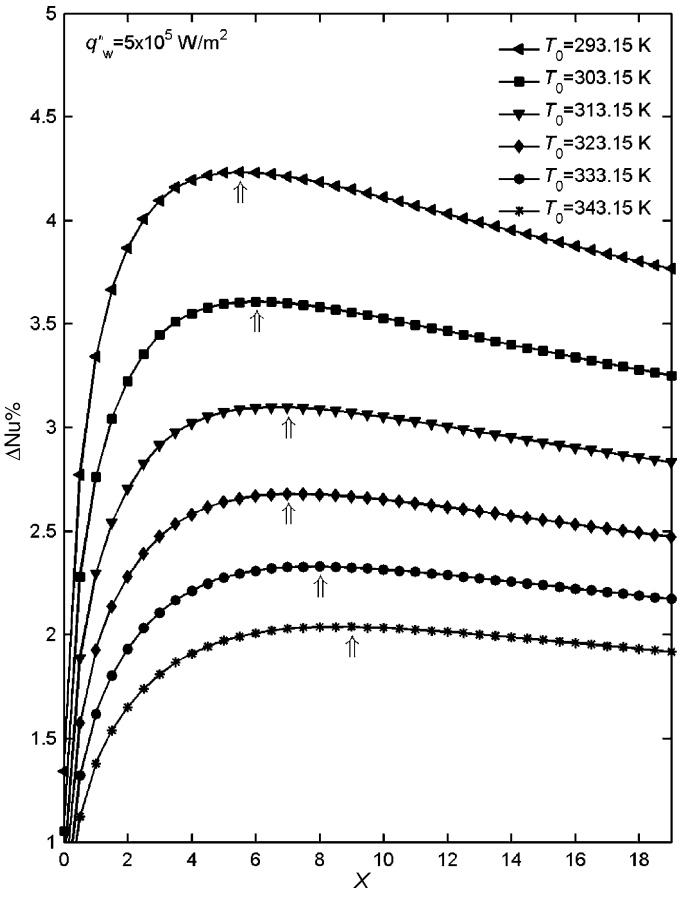

Fig. 6. Effects of inlet temperature T_0 on local $\Delta Nu\%$ at $q''_w = 5 \times 10^5$ W/m^2.

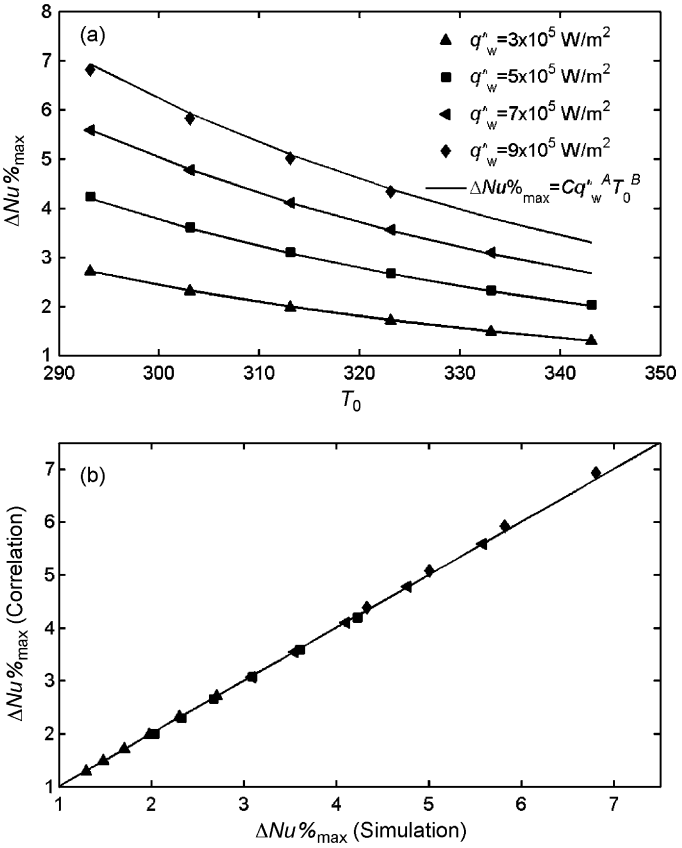

Fig. 7. Comparison of $\Delta Nu\%_{max}$ simulation data with empirical correlation (a) and relative error (b).

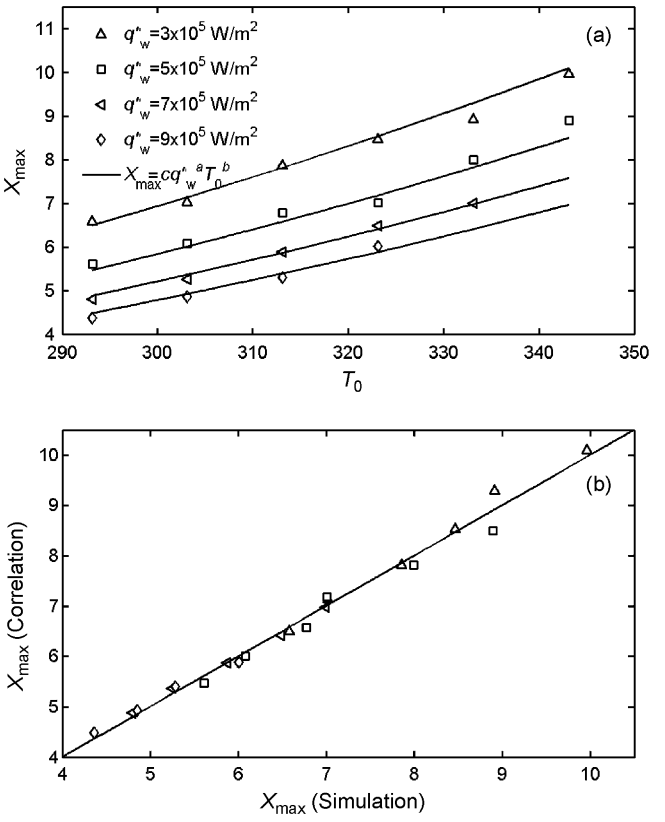

Fig. 8. Comparison of simulated X_{max} with empirical correlation (a) and relative error (b).

the interaction of velocity and temperature fields, as discussed in Section 3.1.

As a successful attempt of theoretical approach, the asymptotic theory method provided the following form of *Nu* correction formula in variable-property problems [12]:

$$\frac{Nu}{Nu_{CP}} = 1 + \varepsilon\left[K_k\bar{h}_B + K_\rho\left(\frac{206}{605} - \frac{232}{1815}\frac{1}{Pr_0}\right) - K_\mu\frac{13}{121} + K_k\frac{148}{605} + K_c\frac{309}{1210}\right] + 0(\varepsilon^2) \quad (15)$$

where $\varepsilon = (11/24)(q''_w R/k_0 T_0)$, $\bar{h}_B = (48/11Pr_0)x$, and $K_\alpha = ((T/\alpha)(d\alpha/dT))_0$ (α as ρ, k, μ or c_p).

In present study, the variation of thermal conductivity and viscosity of liquid water are considered. Following the definition of $\Delta Nu\%$, Eq. (15) is rearranged as

$$\Delta Nu\% = \frac{11}{24}\frac{q''_w R}{k_0 T_0}\left[K_k\frac{48}{11\,Pr_0}x - K_\mu\frac{13}{121} + K_k\frac{148}{605}\right] + 0(\varepsilon^2) \quad (16)$$

For a small heat transfer rate, the second- and higher-order terms are neglected in AT method, which is also called *linear theory* by the author [12]. Such simplification results in a linear relation of $\Delta Nu\% \sim x$, since all parameters remain unchanged for a specified q''_w and T_0 in Eq. (16). A straight forward inference of linear theory is that the variable-property *Nu* enhancement unceasingly amplifies along the flow as long as the fluid is heated. Such phenomenon is apparently not observed in present work, as shown in Sections 3.2 and 4.1. Alternatively, noticeable $\Delta Nu\% \sim x$ peak is detected in every investigated case. It is therefore concluded that for large heat flux conditions (in the range of 10^5 W/m^2), higher-order variable-property deviation over constant property is significant and should be theoretically modeled.

5. Conclusions

A numerical investigation was carried out in present work in an effort to verify the variable-property effect of thermally developing flow in microchannels. Both flow and thermal redevelopment were observed due to the temperature-dependent viscosity and thermal conductivity. Such re-development resulted in marked heat transfer enhancement near the channel wall. The local enhancement behavior was described by defining the peak value and location of relative Nusselt number distribution as $\Delta Nu\%_{max}$ and X_{max}, which reflected the variable-property effect intensity and effective region, respectively. The impacts of heat flux and inlet temperature were discussed. To verify the contributing factors, power-law functions were assumed in the data reduction process at the convenience of discussion, which provided reasonable trend and good accuracy.

The single-peaked $\Delta Nu\% \sim X$ variation in present work disagrees with the linear relation suggested by the asymptotic theory method. The large heat flux and dramatic temperature rise induced higher-order terms of property variation, which was not included in the linear scope of AT method. As a result, strong nonlinear mechanism prevailed in the present relation of $\Delta Nu\%_{max}$ and X_{max}. So far to the authors' knowledge, however, there exists no theoretical solution in literature that successfully solved the high-order variable-property duct flow problems. Then the introduction of peak value and location could be viewed as an attempt to aid the understanding of such kind of problems, which should be quite important in both industrial designing and scientific researches.

Acknowledgement

This investigation is currently supported by the National Natural Science Foundation of China (Grant No. 50636030).

References

[1] D.B. Tuckerman, R.F.W. Pease, High-performance heat sinking for VLSI, IEEE Electron Device Lett. ED-2 (1981) 126–129.
[2] P. Wu, W.A. Little, Measurement of friction factors for the flow of gases in very fine channels used for microminiature Joule–Thomson refrigerators, Cryogenics 23 (1983) 273–277.
[3] P. Wu, W.A. Little, Measurement of the heat transfer characteristics of gas flow in fine channel heat exchangers used for microminiature refrigerators, Cryogenics 24 (1984) 415–420.
[4] J. Pfahler, J. Harley, H. Bau, J. Zemel, Liquid transport in micron and submicron channels, Sens. Actuators A: Phys. 22 (1990) 431–434.
[5] M.M. Rahman, F. Gui, Experimental measurements of fluid flow and heat transfer in microchannel cooling passages in a chip substrate, in: Proceedings of the ASME International Electronics Packaging Conference, ASME, Binghamton, NY, USA, 1993, pp. 685–692.
[6] X.F. Peng, B.X. Wang, Forced convection and flow boiling heat transfer for liquid flowing through microchannels, Int. J. Heat Mass Transf. 36 (1993) 3421–3427.
[7] B.X. Wang, X.F. Peng, Experimental investigation on liquid forced-convection heat transfer through microchannels, Int. J. Heat Mass Transf. 37 (1994) 73–82.
[8] X.F. Peng, G.P. Peterson, Forced convection heat transfer of single-phase binary mixtures through microchannels, Exp. Therm. Fluid Sci. 12 (1996) 98–104.
[9] T.M. Harms, M. Kazmierczak, F.M. Gerner, A. Holke, H.T. Henderson, J. Pilchowski, K. Baker, Experimental investigation of heat transfer and pressure drop through deep microchannels in a (110) silicon substrate, in: Proceedings of the 1997 ASME International Mechanical Engineering Congress and Exposition, ASME, Dallas, TX, USA, 1997, pp. 347–357.
[10] T.M. Adams, S.I. Abdel-Khalik, S.M. Jeter, Z.H. Qureshi, An experimental investigation of single-phase forced convection in microchannels, Int. J. Heat Mass Transf. 41 (1998) 851–857.
[11] R.K. Shah, A.L. London, Laminar flow forced convection in ducts: A Source Book for Compact Heat Exchanger Analytical Data, Academic Press, New York, 1978.
[12] H. Herwig, Effect of variable properties on momentum and heat transfer in a tube with constant heat flux across the wall, Int. J. Heat Mass Transf. 28 (1985) 423–431.
[13] C. Nonino, S. Del Giudice, S. Savino, Temperature dependent viscosity effects on laminar forced convection in the entrance region of straight ducts, Int. J. Heat Mass Transf. 49 (2006) 4469–4481.
[14] S. Del Giudice, C. Nonino, S. Savino, Effects of viscous dissipation and temperature dependent viscosity in thermally and simultaneously developing laminar flows in microchannels, Int. J. Heat Fluid Flow 28 (2007) 15–27.
[15] V. Kumar, P. Gupta, K.D.P. Nigam, Fluid flow and heat transfer in curved tubes with temperature-dependent properties, Ind. Eng. Chem. Res. 46 (2007) 3226–3236.
[16] M.A. Seddeek, A.M. Salem, Further results on the variable viscosity with magnetic field on flow and heat transfer to a continuous moving flat plate, Phys. Lett. A 353 (2006) 337–340.
[17] A. Pantokratoras, Fully developed forced convection of three fluids with variable thermophysical properties flowing through a porous medium channel heated asymmetrically with large temperature differences, J. Porous Media 10 (2007) 409–419.
[18] S.P. Mahulikar, H. Herwig, Theoretical investigation of scaling effects from macro-to-microscale convection due to variations in incompressible fluid properties, Appl. Phys. Lett. 86 (2005) 014105.
[19] S.P. Mahulikar, H. Herwig, Physical effects in laminar microconvection due to variations in incompressible fluid properties, Phys. Fluids 18 (2006) 073601.
[20] H. Herwig, S.P. Mahulikar, Variable property effects in single-phase incompressible flows through microchannels, Int. J. Therm. Sci. 45 (2006) 977–981.
[21] J.-T. Liu, X.-F. Peng, W.-M. Yan, Numerical study of fluid flow and heat transfer in microchannel cooling passages, Int. J. Heat Mass Transf. 50 (2007) 1855–1864.
[22] L. Graetz, Under die Warmeleitungsfahigkeit von Flussigkeiten (On the thermal conductivity of fluids) Part 1, Ann. Phys. Chem. 18 (1883) 79–94.
[23] W. Nusselt, Die Abhangigkeit der Warmeu bergangszahl von der Rohrlange (The relation between heat transmission and length of pipe), Z. Ver. Deutscher Ing. (1910).
[24] F.S. Sherman, Viscous Flow, McGraw-Hill, New York, 1990.
[25] J.P. Holman, Heat Transfer, 8th ed., McGraw-Hill, London, 1997.
[26] V.S. Arpaci, P.S. Larsen, Convection Heat Transfer, Prentice-Hall, London, 1984.